according to

$$\begin{pmatrix}\delta_i \\ \varepsilon_i\end{pmatrix} \sim N\left(\begin{pmatrix}0 \\ 0\end{pmatrix}, \begin{pmatrix}\sigma_{xi}^2 & 0 \\ 0 & \sigma_{zi}^2\end{pmatrix}\right).$$

It is necessary to estimate these variances.

3. PARAMETER ESTIMATION METHOD

In order to find a less-biased parameter estimation method for the model derived in Section 2, we considered expanding Amari and Kawanabe's proposal (1997). They

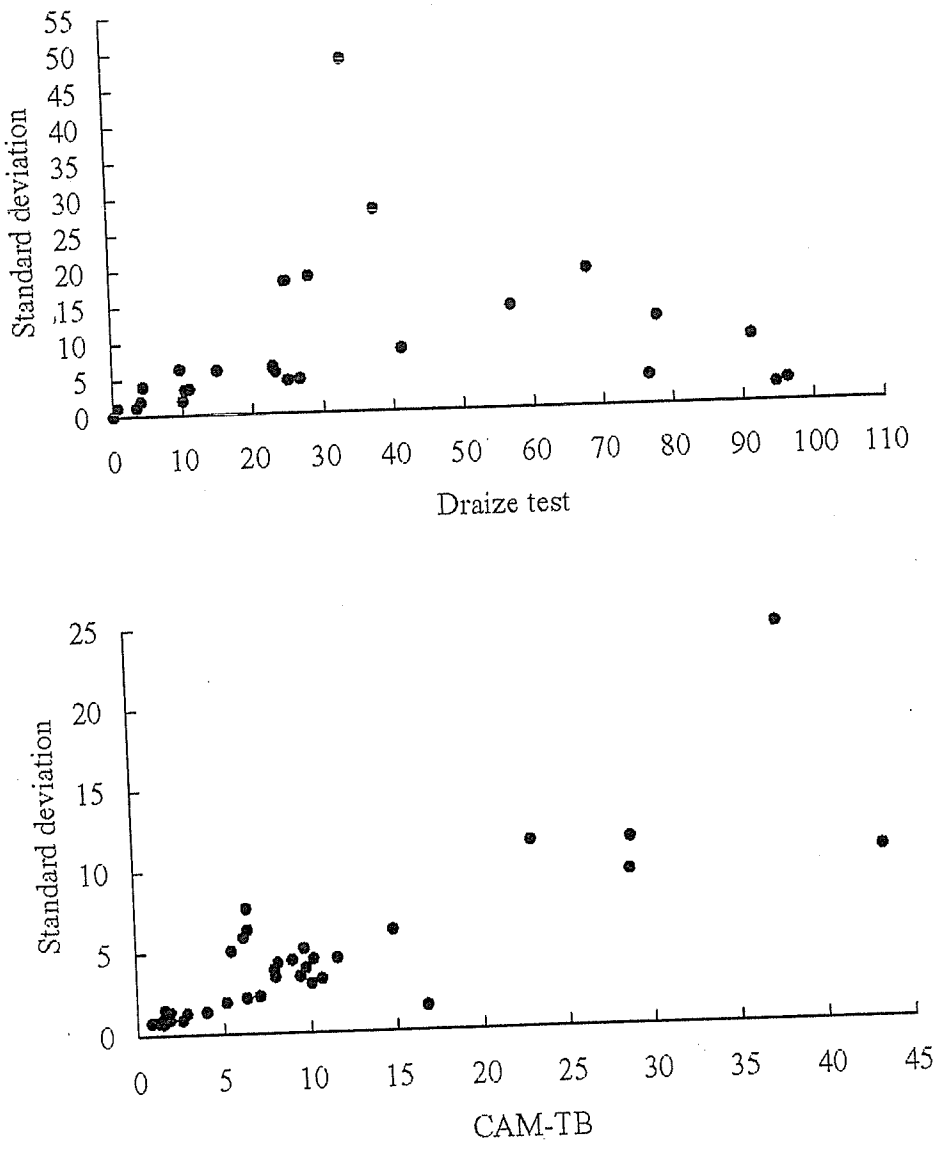

Figure 2. Top: Mean SD plot of the Draize test (vertical axis is standard deviation and horizontal axis is mean). Bottom: Mean SD plot of the CAM-TB (vertical axis is standard deviation and horizontal axis is mean).

discussed the problem that nuisance parameters increase with an increase in sample size. In some cases in which such problems arise, the maximum likelihood method does not derive consistent estimators (e.g., see Neyman and Scott 1948). The statistical analysis of linear measurement error models poses the same problem, that is, nuisance parameters increase with the increase of sample size. For this problem, Amari and Kawanabe (1997) defined a family of estimating functions under the assumption of homogeneous error variances. We extend their method to the case with heterogeneous error variances, and propose a parameter estimation method that makes asymptotic variances of parameters smallest in an extended family of estimating functions.

Under the common known variances, $\sigma_{xi}^2 = \sigma_{zi}^2 = \sigma^2$, Amari and Kawanabe (1997) showed that the estimating functions for β_0 and β_1, $g_0(x, z, \beta)$ and $g_1(x, z, \beta)$, become

$$g_0(x, z, \beta) = \frac{z - \beta_0 - \beta_1 x}{(1 + \beta_1^2)\sigma^2} \tag{3.1}$$

and

$$g_1(x, z, \beta) = h(s)\frac{z - \beta_0 - \beta_1 x}{(1 + \beta_1^2)\sigma^2}, \tag{3.2}$$

where $s = \{x + \beta_1(z - \beta_0)\}/(1 + \beta_1^2)$ is the sufficient statistic for ξ, and $h(s)$ is an arbitrary function of s. The estimating functions (3.1) and (3.2) can produce consistent estimators without depending on nuisance parameters $\xi_1, \ldots, \xi_n$. The asymptotic variance of $\beta_j, j = 0, 1$, a.v.$[\sqrt{n}(\hat{\beta}_j - \beta_j)]$, is given by

$$\text{a.v.}\left[\sqrt{n}\left(\hat{\beta}_j - \beta_j\right)\right] = \frac{\lim_{n\to\infty}(1/n)\sum_{i=1}^n E_{\beta,\xi_i}\left[g_j(x_i, z_i, \beta)^2\right]}{\left\{\lim_{n\to\infty}(1/n)\sum_{i=1}^n E_{\beta,\xi_i}\left[\partial g_j(x_i, z_i, \beta)/\partial\beta_j\right]\right\}^2}, \tag{3.3}$$

where $E_{\beta,\xi_i}[\cdot]$ denotes the expectation with respect to the distributions specified by β and ξ_i, and $\partial g_j(\cdot)/\partial\beta_j$ is the partial derivative with respect to β_j. The derivation of the asymptotic variance (3.3) is given in Appendix A.1.

We extend estimating functions (3.1) and (3.2) to the case with heterogeneous error variances. In order to simplify the estimating equation, we constrained $h(s)$ to a linear function, $h(s) = as + b$. The resulting estimating equations become

$$\sum_{i=1}^n \frac{z_i - \hat{\beta}_0 - \hat{\beta}_1 x_i}{\sigma_{zi}^2 + \hat{\beta}_1^2\sigma_{xi}^2} = 0 \Leftrightarrow \hat{\beta}_0 = \sum_{i=1}^n \frac{z_i - \hat{\beta}_1 x_i}{\sigma_{zi}^2 + \hat{\beta}_1^2\sigma_{xi}^2} \Bigg/ \sum_{i=1}^n \frac{1}{\sigma_{zi}^2 + \hat{\beta}_1^2\sigma_{xi}^2} \tag{3.4}$$

for β_0 and

$$\sum_{i=1}^n \left\{ a_i \frac{\sigma_{zi}^2 x_i + \hat{\beta}_1\sigma_{xi}^2(z_i - \hat{\beta}_0)}{\sigma_{zi}^2 + \hat{\beta}_1^2\sigma_{xi}^2} + b_i \right\} \frac{z_i - \hat{\beta}_0 - \hat{\beta}_1 x_i}{\sigma_{zi}^2 + \hat{\beta}_1^2\sigma_{xi}^2} = 0 \tag{3.5}$$

for β_1. It is necessary to decide on a_i and b_i to estimate $\hat{\beta}_1$, while $\hat{\beta}_0$ is uniquely determined. If we choose a_i and b_i to minimize the asymptotic variance (3.3), we get $a_i = 0$ and $b_i = \xi_i$. Equation (3.5) then becomes

$$\sum_{i=1}^n \xi_i \frac{z_i - \hat{\beta}_0 - \hat{\beta}_1 x_i}{\sigma_{zi}^2 + \hat{\beta}_1^2\sigma_{xi}^2} = 0. \tag{3.6}$$

$\hat{\beta}_1$ cannot be estimated by Equation (3.6) because it includes the unknown parameter ξ_i. Accordingly, we estimate $\hat{\beta}_1$ by substituting the maximum likelihood estimator $\hat{\xi}_i = \left\{\sigma_{zi}^2 x_i + \hat{\beta}_1 \sigma_{xi}^2 (z_i - \hat{\beta}_0)\right\} / (\sigma_{zi}^2 + \hat{\beta}_1^2 \sigma_{xi}^2)$ of ξ_i into Equation (3.6). This $\hat{\xi}_i$ is consistent with the sufficient statistic s_i for ξ_i. As the result, $a_i = 0$ and $b_i = \xi_i$ derive $h(s_i) = s_i$. The estimating equation for β_1 becomes

$$\sum_{i=1}^{n} \frac{\left\{\sigma_{zi}^2 x_i + \hat{\beta}_1 \sigma_{xi}^2 (z_i - \hat{\beta}_0)\right\} (z_i - \hat{\beta}_0 - \hat{\beta}_1 x_i)}{(\sigma_{zi}^2 + \hat{\beta}_1^2 \sigma_{xi}^2)^2}. \tag{3.7}$$

Incidentally, $\hat{\beta}_0$ and $\hat{\beta}_1$ in Equations (3.4) and (3.7) are the same as the maximum likelihood estimators (Walter 1997). The derivations of Equations (3.4) and (3.7) through the maximum likelihood method are given in Appendix A.2. The variances of $\hat{\beta}_0$ and $\hat{\beta}_1$ are given by

$$\begin{aligned} \mathrm{var}(\hat{\beta}_0) &= \frac{\sum f_i \xi_i^2}{\sum f_i \sum f_i \xi_i^2 - \left(\sum f_i \xi_i\right)^2} \\ \mathrm{var}(\hat{\beta}_1) &= \frac{\sum f_i}{\sum f_i \sum f_i \xi_i^2 - \left(\sum f_i \xi_i\right)^2}, \end{aligned}$$

where $f_i = 1/(\sigma_{zi}^2 + \beta_1^2 \sigma_{xi}^2)$ and $\sum = \sum_{i=1}^{n}$.

4. SIMULATION STUDY

We conducted a simulation study to evaluate the performance of the parameter estimation method proposed in Section 3. The simulation study was conducted in a framework that was adaptable to data obtained in a validation study described in Section 2. The following four parameter estimation methods were compared:

1. Ordinary least squares (we call this method OLS).
2. Estimating Equations (3.4) and (3.7) under the assumption of homogeneous error variances, and the error variance of response variables are equal to that of explanatory variables, that is, $\sigma_{xi}^2 = \sigma_{zi}^2 = \sigma^2$ (we call this method EV1).
3. Estimating Equations (3.4) and (3.7) under the assumption of homogeneous error variances, and the error variance of response variables are not equal to that of explanatory variables, that is, $\sigma_{xi}^2 = \sigma_x^2$ and $\sigma_{zi}^2 = \sigma_z^2$ (we call this method EV2).
4. Estimating Equations (3.4) and (3.7) under the assumption of heterogeneous error variances, and all error variances of response variables and explanatory variables vary between measurements (we call this method NEV).

We substituted the Equation (3.4) into Equation (3.7) to find $\hat{\beta}_1$ in EV1, EV2, and NEV. The Newton-Raphson algorithm was used to solve estimating equations. The initial values were set to be OLS estimates. The conditions and steps for the simulation study were as follows:

1. Generate a uniform random number with a range between 5 and 15. This value is set as ξ, which denotes a true measurement in the CAM-TB.

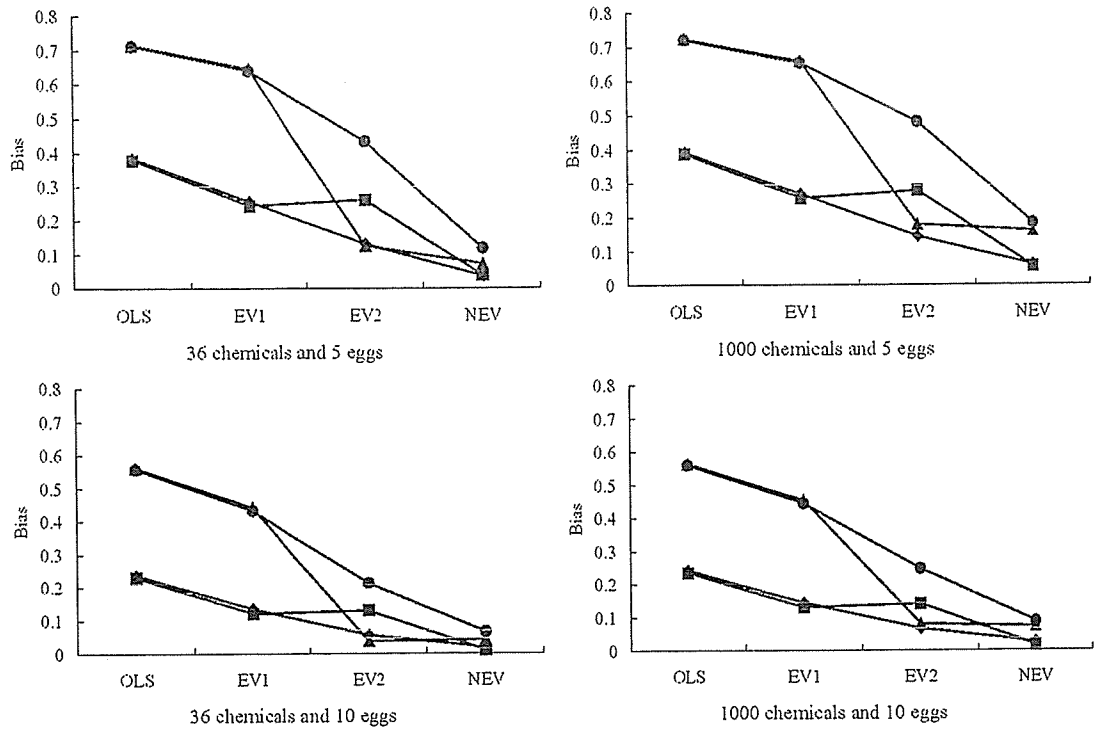

Figure 3. The Results of $\hat{\beta}_1$ for a Simulation Study: Biases (true values minus the means of estimates). Diamonds: $(SD_x, SD_y) = (.5\xi, .0025\,\eta(110-\eta))$, squares: $(SD_x, SD_y) = (.5\xi, .005\,\eta(110-\eta))$, triangles: $(SD_x, SD_y) = (\xi, .0025\,\eta(110-\eta))$, and circles: $(SD_x, SD_y) = (\xi, .005\,\eta(110-\eta))$.

2. Calculate $\eta = 110\exp(\xi - 10)/\{1 + \exp(\xi - 10)\}$ (true model). This η denotes a true score in the Draize test.
3. Generate normal random numbers with mean ξ and standard deviation $\mathrm{SD}_x = .5\,\xi$ or ξ. The number of generated random numbers is 5 or 10, which is assumed to be the number of eggs used in the CAM-TB. Set the mean and standard deviation calculated from these random numbers as a measurement and its according standard deviation in the CAM-TB. Similarly, generate normal random numbers with mean η and standard deviation $\mathrm{SD}_y = .0025\eta(110-\eta)$ or $.005\eta(110-\eta)$. If a generated value is smaller than 0 or larger than 110, the value is replaced with 0 or 110. The number of generated random numbers is 3, which is the same as the number of rabbits used in the Draize test. Set the mean and standard deviation calculated from these random numbers as the score and its according standard deviation in the Draize test.
4. Repeat Steps 1–3 36 times (in correlation to the number of chemical substances) or 1,000 times. This yields one dataset.
5. Estimate parameters (β_0 and β_1) by the four methods described (OLS, EV1, EV2, and NEV).
6. Repeat the above steps 1,000 times, and calculate means, biases (true values minus means), and mean squared errors (MSEs) of parameter estimates ($\hat{\beta}_0$ and $\hat{\beta}_1$).

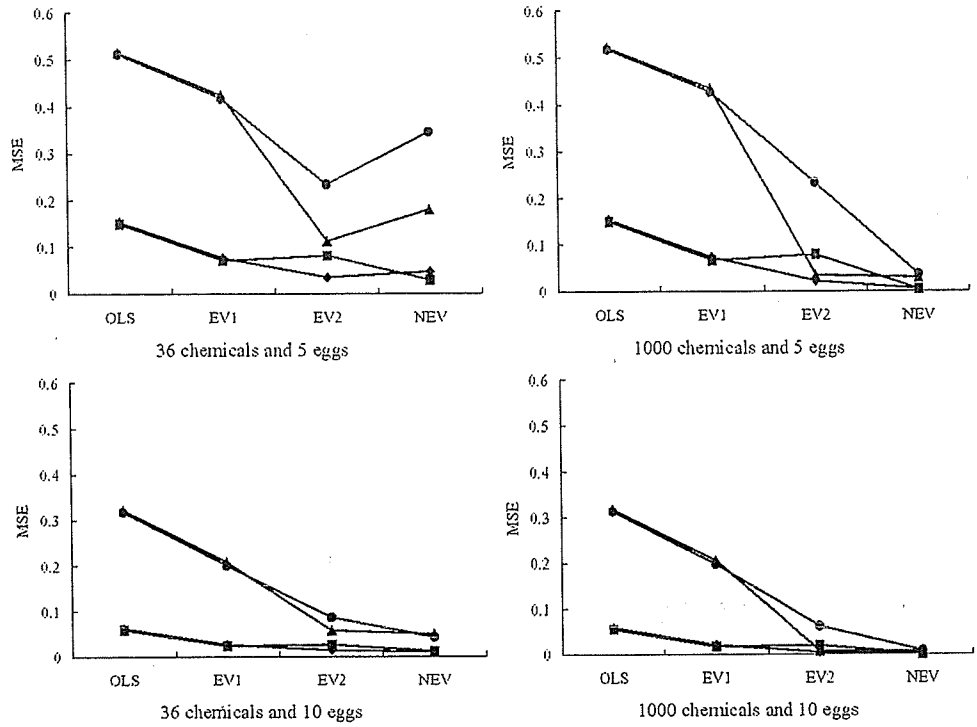

Figure 4. The Results of $\hat{\beta}_1$ for a Simulation Study: Mean squared errors. Diamonds: $(SD_x, SD_y) = (.5\xi, .0025\eta(110-\eta))$, squares: $(SD_x, SD_y) = (.5\xi, .005\eta(110-\eta))$, triangles: $(SD_x, SD_y) = (\xi, .0025\eta(110-\eta))$, and circles: $(SD_x, SD_y) = (\xi, .005\eta(110-\eta))$.

The results of the simulation study are summarized in Figures 3 and 4. We show only the results of $\hat{\beta}_1$ since $\hat{\beta}_0$ was uniquely determined as a result of $\hat{\beta}_1$. Figure 3 indicates biases on the four methods under $4 \times 2 \times 2 = 16$ conditions (pairs of standard deviations $(\mathrm{SD}_x, \mathrm{SD}_y) = (.5\xi, .0025\eta(110-\eta))$, $(.5\xi, .005\eta(110-\eta))$, $(\xi, .0025\eta(110-\eta))$ or $(\xi, .005\eta(110-\eta))$; the number of chemical substances = 36 or 1,000; and the number of eggs = 5 or 10). Figure 4 indicates mean squared errors.

The following results were obtained from Figure 3. First, magnitude of biases for the four methods was examined. All four results in Figure 3 show that NEV, EV2, EV1, and OLS generated smaller order biases. However, the biases of EV2 are a little larger than those of EV1 under $(\mathrm{SD}_x, \mathrm{SD}_y) = (.5\xi, .005\eta(110-\eta))$ (symbols in Figure 3 = squares). The biases of EV2 are also similar to those of NEV under $(\mathrm{SD}_x, \mathrm{SD}_y) = (\xi, .0025\eta(110-\eta))$ (symbols in Figure 3 = triangles).

Second, we examined how the difference of standard deviations (SD_x or SD_y) influenced biases. All four results in Figure 3 show that biases for $\mathrm{SD}_x = \xi$ (symbols in Figure 3 = triangles and circles) are larger than those for $\mathrm{SD}_x = .5\xi$ (symbols in Figure 3 = diamonds and squares). On the other hand, the difference of SD_y, that is, $\mathrm{SD}_y = .0025\eta(110-\eta)$ (symbols in Figure 3 = diamonds and triangles) or $\mathrm{SD}_y = .005\eta(110-\eta)$ (symbols in Figure 3 = squares and circles), does not generate much difference in biases except for EV2. These results imply that error variances in the CAM-TB have more influence on biases than those of the Draize test. This is especially true for OLS and EV1. It seems that

Table 1. Parameter Estimates and Their Standard Errors by Four Estimation Methods (OLS: ordinary least squares; EV1: $\sigma^2_{xi} = \sigma^2_{zi} = \sigma^2$; EV2: $\sigma^2_{xi} = \sigma^2_x$ and $\sigma^2_{zi} = \sigma^2_z$ but $\sigma^2_x \neq \sigma^2_z$; and NEV: all error variances vary between measurements)

	$\hat{\beta}_0$	s.e. ($\hat{\beta}_0$)	$\hat{\beta}_1$	s.e. ($\hat{\beta}_1$)
OLS	−6.189	.673	.277	.047
EV1	−6.399	1.393	.298	.098
EV2	−6.281	1.633	.287	.114
NEV	−10.619	.380	.864	.150

error variances in the Draize test have no relevance to biases. However, the biases of EV2 are small when error variances in the CAM-TB are large.

Third, we examined how differences in the numbers of chemical substances or the number of eggs influenced biases. The comparisons between the same numbers of chemical substances and different numbers of eggs (the comparisons between top and bottom in Figure 3) show that on all of four methods, biases when the number of eggs = 5 are larger than those for when the number of eggs = 10. On the other hand, the comparisons between the different numbers of chemical substances and same numbers of eggs (the comparisons between left and right in Figure 3) show that the magnitude of bias does not change with changes in the number of chemical substances. These results imply that biases become smaller if the number of eggs used in the CAM-TB increases but not smaller even if the number of chemical substances increases.

In Figure 4, we can see that MSEs also have features similar to biases. However, NEV produces large MSEs in the case in which the number of chemical substances is 36 and the number of eggs is 5.

5. APPLICATION OF THE PROPOSED METHOD TO REAL DATA

We applied the proposed method and the other 3 methods to the data described in Section 2.

Table 1 summarizes the regression parameters and their standard errors estimated by the four methods described in Section 3. Figure 5 shows their fitted curves. $\hat{\beta}_0$ and $\hat{\beta}_1$ by OLS, EV1, and EV2 (solid line, large broken line, and small broken line in Figure 5) provided almost identical results. Those provided by NEV (solid thin line in Figure 5) were considerably differed from the other three methods. As Figure 5 indicates, the four methods do not fit the data well.

Our objective is to formulate a model to predict the score in the Draize test by the measurement in the CAM-TB. Accurate prediction of Draize test scores is much more important when CAM-TB produces moderate measurements. Large CAM-TB measurements indicate high Draize test scores, even though the prediction is not very precise. Though the prediction is loose, it is possible to identify chemical substances that have strong toxicity. A chemical substance having strong toxicity cannot be adopted for use in cosmetics. When the CAM-TB test produces moderate measurements, however, we should be careful to avoid underestimating the toxicity of the chemical substance being tested. This is what happens

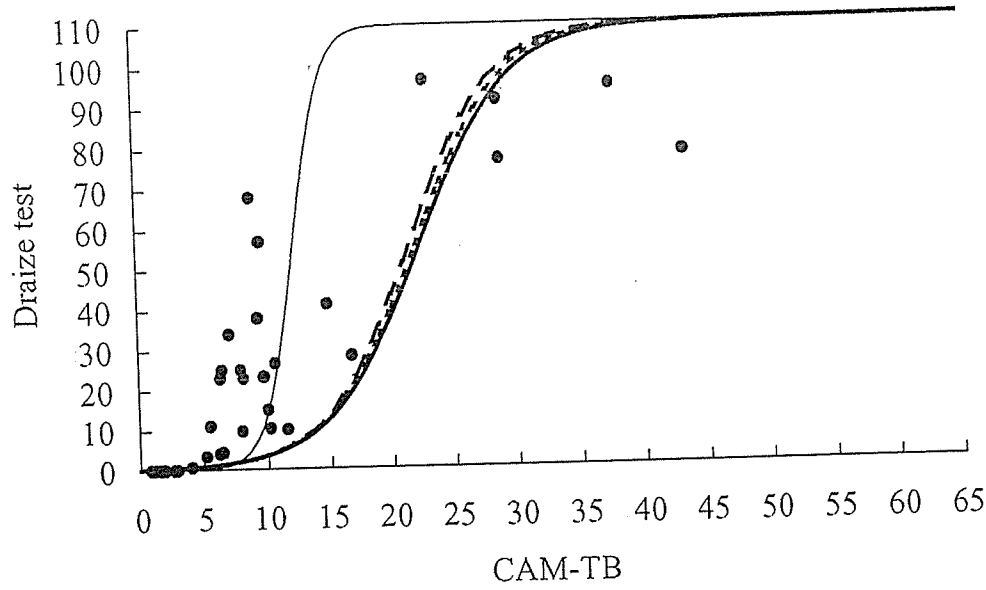

Figure 5. Fitted curves (solid line: OLS, large broken line: EV1, small broken line: EV2, and solid thin line: NEV).

when the score in the Draize test is underestimated.

Figure 5 shows that OLS, EV1, and EV2 underestimate the score in the Draize test when the CAM-TB test produces moderate measurements. Figure 5 also shows that NEV makes the degree of underestimation smaller in the moderate measurements in comparison with the other three methods. NEV is a worse fit than the other three methods for large measurements. As discussed earlier, however, it is not important that the fit for these measurements is wrong. Consequently, we consider that the proposed method, NEV, results in a better prediction formula than the other three methods.

6. DISCUSSION

In this article, we extended the estimating function method proposed by Amari and Kawanabe (1997) to the case in which error variances vary between measurements. The estimators for the proposed method were incidentally identical to the maximum likelihood estimators.

We also conducted a simulation study to compare the regression parameters estimated by the proposed method with those estimated by three other methods under the assumption of homogeneous error variances. The parameters estimated by the proposed method, NEV, may be imprecise when sample size is small and error variances are large. However, the results of the simulation study suggest that, in comparison to the other three methods, NEV results in smaller biases and MSEs. As shown in Figure 4, NEV produced large MSE in the case in which the number of chemical substances was 36 and the number of eggs was 5. The reason is that there are few cases in which NEV takes a very large value of $\hat{\beta}_1$ when the error variances are large. For example, under $(\mathrm{SD}_x, \mathrm{SD}_y) = (\xi, .005\eta(110-\eta))$, NEV took 16.93 as the maximum value of $\hat{\beta}_1$.

In the simulation study, normal random numbers were generated on the original scales before the logit transformation, while the scales after the logit transformation were modeled. Our primary objective was to see if the proposed method could have worked in the validation study. In the validation study, measurement errors occurred at the original scale. This was because we considered normal error structures at the original scale in the simulation study. If we knew the true error structures, it would be appropriate to use a nonlinear measurement error model. Note that to develop such a nonlinear measurement error model is troublesome with heterogeneous error variances. As a result, in the simulation study, we used somewhat misspecified models. Nevertheless, the simulation study showed that the proposed method, NEV, gave the smaller biases and MSEs than the other three methods.

The goal of the validation study was to predict Draize test scores from CAM-TB values. When a fitted curve shows greater deviation in the direction of underestimating the score in the Draize test, there is a greater risk of underestimating a chemical substance's toxicity. From the results of the simulation study shown in Section 3, it is reasonable to conclude that the proposed method is less biased than the other three methods in the validation study. The results of the simulation study also indicate that we can make bias and MSE smaller if larger numbers of eggs are used in the CAM-TB. This shows that if alternative methods such as the CAM-TB are carried out with large numbers of experiment materials for each chemical substance, we can estimate the regression parameters more precisely.

In validation studies, both the measurements in animal experiments and in alternative methods are measured with error. We need to adopt measurement error models when we predict measurements in animal experiments by alternative methods. In order to investigate whether or not the method proposed in this paper is useful in evaluating alternative methods, we need to examine other alternative methods in addition to CAM-TB.

APPENDIX

A.1 THE DERIVATION OF ASYMPTOTIC VARIANCE (3.3)

If the estimating equation for $\hat{\beta}_j (j = 0, 1)$, $\sum_{i=1}^{n} g_j(x_i, z_i, \hat{\beta}_j, \beta_k) = 0\,(j \neq k)$, is expanded with a Taylor series on the true parameter β_j, we get

$$0 = \sum_{i=1}^{n} g\left(x_i, z_i, \beta\right) + \sum_{i=1}^{n} \frac{\partial g(x_i, z_i, \beta)}{\partial \beta_j} \left(\hat{\beta}_j - \beta_j\right) + O_p\left(\left|\hat{\beta}_j - \beta_j\right|^2\right). \tag{A.1}$$

$\hat{\beta}_j$ takes the almost same value as β_j when n becomes very large. Then, since the higher order terms, $O_p\left(\left|\hat{\beta}_j - \beta_j\right|^2\right)$, are negligible, Equation (A.1) is transformed as

$$\sqrt{n}\left(\hat{\beta}_j - \beta_j\right) = -\frac{1}{\sqrt{n}} \sum_{i=1}^{n} g\left(x_i, z_i, \beta\right) \Bigg/ \frac{1}{n} \sum_{i=1}^{n} \frac{\partial g\left(x_i, z_i, \beta\right)}{\partial \beta_j}. \tag{A.2}$$

By applying the law of large numbers, the denominator on the right hand side in Equation (A.2) converges to

$$\lim_{n\to\infty}\frac{1}{n}\sum_{i=1}^{n}E_{\beta,\xi_i}\left[\frac{\partial g_j(x_i,z_i,\beta)}{\partial\beta_j}\right].$$

By the central limit theorem, the numerator on the right hand side in Equation (A.2) is distributed according to

$$\frac{1}{\sqrt{n}}\sum_{i=1}^{n}g_j(x_i,z_i,\beta)\sim N\left(0,E_{\beta,\xi_i}\left[g_j(x_i,z_i,\beta)^2\right]\right).$$

Therefore, $\hat{\beta}_j$ is also asymptotically normally distributed with the asymptotic variance

$$\text{a.v.}\left[\sqrt{n}\left(\hat{\beta}_j-\beta_j\right)\right]=\frac{\lim_{n\to\infty}(1/n)\sum_{i=1}^{n}E_{\beta,\xi_i}\left[g_j(x_i,z_i,\beta)^2\right]}{\left\{\lim_{n\to\infty}(1/n)\sum_{i=1}^{n}E_{\beta,\xi_i}\left[\partial g_j(x_i,z_i,\beta)/\partial\beta_j\right]\right\}^2}.$$

A.2 THE DERIVATIONS OF EQUATIONS (3.4) AND (3.7) THROUGH THE MAXIMUM LIKELIHOOD METHOD

A pair of measurements, (x_i,z_i), $i=1,2,\ldots,n$, have a functional relationship

$$\begin{aligned}x_i &= \xi_i+\delta_i\\ z_i &= \beta_0+\beta_1\xi_i+\varepsilon_i,\end{aligned}$$

where δ_i and ε_i are distributed according to

$$\begin{pmatrix}\delta_i\\ \varepsilon_i\end{pmatrix}\sim N\left(\begin{pmatrix}0\\ 0\end{pmatrix},\begin{pmatrix}\sigma_{xi}^2 & 0\\ 0 & \sigma_{zi}^2\end{pmatrix}\right).$$

The log-likelihood function, $\log L$, is given as

$$\log L=C-\frac{1}{2}\sum_{i=1}^{n}\left\{\frac{(x_i-\xi_i)^2}{\sigma_{xi}^2}+\frac{(z_i-\beta_0-\beta_1\xi_i)^2}{\sigma_{zi}^2}\right\},$$

where C denotes a set of constant terms that does not depend on the parameters β_0,β_1, and ξ_i. $\partial\log L/\partial\xi_i=0$ gives the maximum likelihood estimator

$$\hat{\xi}_i=\frac{\sigma_{zi}^2x_i+\hat{\beta}_1\sigma_{xi}^2(z_i-\hat{\beta}_0)}{\sigma_{zi}^2+\hat{\beta}_1^2\sigma_{xi}^2}.$$

By substituting this $\hat{\xi}_i$ into $\partial\log L/\partial\beta_0=0$ and $\partial\log L/\partial\beta_1=0$, Equations (3.4) and (3.7) are derived.

ACKNOWLEDGMENTS

The authors thank Takashi Omori and the referees for their helpful comments.

[Received February 2004. Revised May 2004.]

REFERENCES

Amari, S., and Kawanabe, M. (1997), "Information Geometry of Estimating Functions in Semi-Parametric Statistical Models," *Bernoulli*, 3, 29–54.

Draize, J., Woodard, G., and Galvery, H. (1944), "Methods for the Study of Irritation and Toxicity of Substances Applied Topically to the Skin and Mucous Membranes," *The Journal of Pharmacology and Experimental Therapeutics*, 82, 377–390.

Fuller, W. A. (1987), *Measurement Error Models*, New York: Wiley.

Hagino, S., Itagaki, H., Kato, S., and Kobayashi, T. (1993), "Further Evaluation of the Quantitative Chorioallantoic Membrane Test Using Trypan Blue Stain to Predict the Eye Irritancy of Chemicals," *Toxicology in Vitro*, 7, 35–39.

Hagino, S., Itagaki, H., Kato, S., Kobayashi, T., and Tanaka, M. (1991), "Quantitative Evaluation to Predict the Eye Irritancy of Chemicals Modification of Chorioallantoic Membrane Test by Using Trypan Blue," *Toxicology in Vitro*, 5, 301–304.

Hagino, S., Kinoshita, S., Tani, N., Nakamura, T., Ono, N., Konishi, K., Iimura, H., Kojima, H., and Ohno, Y. (1999), "Interlaboratory Validation of In Vitro Eye Irritation Tests for Cosmetic Ingredients (2) Chorioallantoic Membrane (CAM) Test," *Toxicology in Vitro*, 13, 99–113.

Japan Cosmetic Industry Association (1994), *Report of the First Validation Study on Alternative Methods to the Draize Eye Irritation Test*, Japan Cosmetic Industry Association (in Japanese).

Neyman, J., and Scott, E. L. (1948), "Consistent Estimates Based on Partly Consistent Observation," *Econometrica*, 32, 1–32.

OECD Test Guidelines Programme (1996), "Options for a Testing Strategy for the Testing of Skin and Eye Irritancy," Final report of the OECD Workshop on Harmonization of Validation and Acceptance Criteria for Alternative Toxicological Test Methods, September 18–19, 1996, the Chateau de la Muette, Paris.

Walter, S. D. (1997), "Variation in Baseline Risk as an Explanation of Heterogeneity in Meta-analysis," *Statistics in Medicine*, 16, 2883–2900.

Wilhelmus, K. R. (2001), "The Draize Eye Test," *Survey of Ophthalmology*, 45, 493–515.

Journal of Dermatological Science (2006) 41, 127–136

ELSEVIER

Journal of Dermatological SCIENCE

www.intl.elsevierhealth.com/journals/jods

Establishment of murine model of allergic photocontact dermatitis to ketoprofen and characterization of pathogenic T cells

Satoshi Imai [a,b], Kenji Atarashi [a,b], Koichi Ikesue [b], Katsuhiko Akiyama [b], Yoshiki Tokura [a,*]

[a] *Department of Dermatology, University of Occupational and Environmental Health, 1-1 Iseigaoka, Yahatanishi-ku, Kitakyushu 807-8555, Japan*
[b] *Fundamental Research Laboratories, Hisamitsu Pharmaceutical Co. Inc., Tsukuba, Japan*

Received 9 June 2005; received in revised form 17 August 2005; accepted 26 August 2005

KEYWORDS
Photocontact dermatitis;
Contact photoallergy;
Ketoprofen;
Chemokine

Summary

Background: Ketoprofen is well known to evoke the allergic type of photocontact dermatitis when it is applied to the skin and irradiated with ultraviolet A (UVA) light.
Objective: We aimed to establish a murine model of this photosensitivity and to characterize pathogenic T cells concerned with the sensitivity.
Methods: Various strains of mice were sensitized on two consecutive days by application of ketoprofen to the shaved abdomen and irradiation of the skin with UVA. Five days later, they were elicited with ketoprofen plus UVA on the earlobes. Immune lymph node cells and epidermal cells from the challenged sites were analyzed by RT-PCR.
Results: Mice were successfully sensitized and challenged with 4% and 2% ketoprofen, respective, plus UVA at20 J/cm^2. The responses in H-2^k mice were higher than those in the other strains examined. Immune lymph node CD4$^+$ or CD8$^+$ cells from ketoprofen-photosensitized H-2^k mice were transferred i.v. to naïve syngeneic recipients. Mice receiving CD4$^+$ but not CD8$^+$ cells exhibited ketoprofen photosensitivity, but transference of both CD4$^+$ and CD8$^+$ cell populations was more effective. Lymph node cells from photosensitized mice expressed high levels of mRNA for Th2 cytokine (IL-4) and Th2 chemokine receptor (CCR4) as well as Th1 cytokine (IFN-γ) and Th1 chemokine receptor (CXCR3), as assessed by RT-PCR. In addition, epidermal cells from challenged earlobes expressed increased levels of both Th1 (TARC) and Th2 (Mig) chemokines.
Conclusion: It is considered that not only Th1 but also Th2 cells participate in the pathogenesis of murine photocontact dermatitis to ketoprofen.

* Corresponding author. Tel.: +81 93 691 7445; fax: +81 93 691 0907.
E-mail address: tokura@med.uoeh-u.ac.jp (Y. Tokura).

0923-1811/$30.00
doi:10.1016/j.jdermsci.2005.08.006

1. Introduction

Photocontact dermatitis is a specialized form of contact dermatitis evoked by various chemicals, such as halogenated salicylanilides, musk ambrette, benzophenone-3 (oxybenzone), and non-steroidal anti-inflammatory drugs [1]. Patients develop dermatitis, when their skin is exposed to these agents and subsequent ultraviolet (UV) light. This disorder is pathohysiologically divided into two types, phototoxic and photoallergic ones. While the phototoxic dermatitis is mediated by oxygen intermediates, the photoallergic type, also known as contact photosensitivity, is a well-organized cutaneous sensitivity that is immunologically induced and elicited with photoallergic agent and UVA. Recently, the incidence of the photoallergic type is higher than the phototoxic one, because the major causative agents are non-steroidal anti-inflammatory drug with photoallergic properties [2].

It has been clarified that the majority of photoallergic agents are photohaptens, which bind covalently to protein via the formation of free radicals resulting from UV irradiation [2]. Because of this photobinding ability, cells are easily photomodified with photohapten under exposure to UVA, which is the action spectrum of photocontact dermatitis. The main sequential events in photocontact dermatitis have been investigated with 3,3′,4′,5-tetrachlorosalicylanilide (TCSA) in mice [3,4] and are virtually the same as those of ordinary contact dermatitis except for the requirement of UV irradiation in sensitization and challenge. Photoconjugation of epidermal cells with TCSA is the initial step. Langerhans cells (LC), which are professional antigen-presenting cells in the epidermis, play an important role. Photohapten-bearing LC migrates to draining lymph nodes in the sensitization phase [5]. T cells sensitized by photohapten-bearing LC induce the photosensitivity [3] and suppressor or regulatory T cells involved in this sensitivity have been identified [6].

Ketoprofen (KP), widely used as a topical non-steroidal anti-inflammatory drug, is clinically well known to induce the allergic type of photocontact dermatitis [7–11]. In addition to the high incidence of occurrence of photocontact dermatitis, KP is an interesting drug in its cross-photoreactivity with thiaprofenic acid, suprofen, phenofibrate, and benzophenone-3 [7–11]. These substances have a photohaptenic moiety [2] as well as a phototoxic ability [12,13].

A model of KP photocontact dermatitis has been reported using guinea pigs [11]. However, little is known regarding the immunological characteristics of photocontact dermatitis to KP. In this study, we established a murine model of KP photosensitivity and investigated the immunological mechanism, focusing on the involvement of Th1 and Th2 cells.

2. Materials and methods

2.1. Animals

AKR/N (H-2^k), CBA/J (H-2^k), C3H/He (H-2^k), BALB/c (H-2^d), DBA/2 (H-2^d), A/J (H-2^a), C57BL/6 (B6; H-2^b) were obtained from Kyudo Co. Ltd. (Kumamoto, Japan). BALB.K/Ola (H-2^k) mice were kindly provided by National Institute of Genetics (Mishima, Japan). Female mice, 8-week old, were used in this study.

2.2. Chemicals

KP was obtained from Hisamitsu Pharmaceutical Co. Inc. (Tokyo, Japan) and 3,3′,4′,5-tetrachlorosalicylanilide (TCSA) was purchased from Kanto Chemical Co. Inc. (Tokyo, Japan).

2.3. Light source

Black light (FL20SBL-B) emitting UVA ranging from 320 to 400 nm with a peak emission at 365 nm was purchased from Toshiba Electric Co. (Tokyo, Japan). With a UV radiometer (Topcon Technohouse Corp., Tokyo, Japan), the energy output of three 20 W tubes of black light at a distance of 20 cm was 2.4 mW/cm^2 at 365 nm and 0.17 mW/cm^2 at 305 nm.

2.4. Photosensitization and photochallenge to KP

The basic method for photosesitization and photochallenge was described previously [3,4]. Mice were painted with 50 μl of 1, 2 or 4% KP in acetone to the clipped abdomen. Within 30 min, the painted site was irradiated with three tubes of black light at a distance of 20 cm for 2.5 h (20 J/cm^2 at 365 nm) unless otherwise mentioned by placing cages containing mice over the lights. We used a pane of window glass 3 mm thick to insure that no radiation below 320 nm reached the skin. The painting plus irradiation was performed on two consecutive days, i.e., days 0 and 1. Before challenge, the basal line thickness of both ears on all mice was measured with a dial thickness gauge. On day 5, all mice were challenged on both sides of each earlobe with 25 μl of 2% KP in ethanol unless otherwise described. Within 30 min, the mice received irradiation under black light at a distance of 20 cm at 20 J/cm^2 at

365 nm. Ear thickness was measured 24 h after irradiation and was expressed as the mean increment in thickness above basal line control value.

2.5. Preparation of single cell suspension of lymph node cells (LNC) and epidermal cells

Axillary and inguinal lymph nodes were collected on day 3 or 5 from mice photosensitized with KP on days 0 and 1. Single cell suspensions were prepared by teasing lymph nodes. For preparation of epidermal cells, excised murine earlobes were incubated in 0.2% trypsin. Epidermal cells were dispersed and washed three times in PBS, as described previously [14].

2.6. Adoptive transfer of sensitivity with immune LNC

Immune LNC were prepared on day 5 from KP-photosensitized AKR/N mice. To obtain purified $CD4^+$ or $CD8^+$ T cells, LNC were incubated with anti-CD4 or anti-CD8 monoclonal antibody (mAb)-conjugated magnetic beads (Dynal Inc., Oslo, Norway) and the bound cells were detached from the beads with Detachabeads (Dynal Inc.) according to the manufacture's directions. Unfractionated LNC (2×10^7 cells/mouse) or varying ratios of $CD4^+$ or $CD8^+$ T cells in 0.4 ml of phosphate buffered saline (PBS; pH 7.4) were injected i.v. into naïve recipients. The control mice were injected with PBS alone. Within 1 h after cell transfer, the recipient and control mice were challenged on the ears with 2% KP plus 20 J/cm^2 UVA, and ear swelling response was measured after 24 h. In a comparison, BALB/c mice were sensitized with 1% TCSA plus 12 J/cm^2 UVA on days 0 and 1, as described previously [3,4], and LNC were transferred to naïve syngeneic mice. Epicutaneous sensitization and challenge with TCSA plus UVA was reported [3].

2.7. Reverse transcription-polymerase chain reaction (RT-PCR) assay

Total RNA was extracted from LNC or epidermal cells using the SVTotal RNA Isolation system (Promega Co., Madison, WI, USA). To prepare first strand cDNA, 1 μg of RNA was incubated in 100 μl of buffer containing 10 mM dithiothreitol, 2.5 mM $MgCl_2$, dNTP mix, 200 U of reverse transcriptase II (Invitorogen, Carlsbad, CA, USA) and 0.1 mM oligo $(dT)_{12-18}$ (Invitorogen). Each cDNA were amplified in a 50 μl PCR solution containing 0.8 mM $MgCl_2$, dNTP mix and DNA polymerase (Roche Applied Science, Penzberg, Germany) with synthesized primers. Samples were heated to 95 °C for 2 min, 55 °C for 2 min and 72 °C for 3 min, and cycled 40 times through 95 °C for 1 min, 55 °C for 2 min and 72 °C for 3 min. The final incubation was 72 °C for 7 min. The mixture was subjected to 1% agarose gel for electrophoresis with the indicated markers and primers for the internal standard β-actin. Each sample was applied more than two lanes in the same gel. The agarose gel was stained with ethidium bromide and photographed with UV transillumination.

The sense/antisense primer sequences were as follows. Interferon-γ (IFN-γ): 5′-TGA ACG CTA CAC ACT GCA TCT TGG-3′ and 5′-CGA CTC CTT TTC CGC TTC CTG AG-3′; IL-4: 5′-ATG GGT CTC AAC CCC CAG CTA GT-3′ and 5′-GCT CTT TAG GCT TTC CAG GAA GTC-3′; CXCR3: 5′-GCC GAT GTT CTG CTG GTG TTA A-3′ and 5′-TTT TCG ACC ACA GTT GCG GGC-3′ CCR4: 5′-TCG GAT TTG CTG TTC GTC CTG T-3′ and 5′-TAA GGC AGC AGT GAA TGA AGC C-3′; IP-10; 5′-CGC ACC TCC ACA TAG CTT ACA G-3′ and 5′-CCT ATC CTG CCC ACG TGT TGA G-3′; Mig: 5′-TGA TAA GGA ATG CAC GAT GCT C-3′ and 5′-TTC CTT GAA CGA CGA CGA CTT T-3′; TARC: 5′-CAG GAA GTT GGT GAG CTG GTA TAA-3′ and 5′-TTG TGT TCG CCT GTA GTG CAT A-3′; MDC: 5′-TCT GAT GCA GGT CCC TAT GGT-3′ and 5′-TTA TGG AGT AGC TTC TTC ACC CAG-3′; β-actin: 5′-TGG AAT CCT GTG GCA TCC ATG AAA C-3′ and 5′-TAA AAC GCA GCT CAG TAA CAG TCC G-3′.

2.8. Statistical analysis

Student's *t*-test was employed to examine the significance between the means, and $p < 0.05$ was considered statistically significant.

3. Results

3.1. Induction of photocontact dermatitis by KP plus UVA

As shown in Fig. 1, AKR/N mice were sensitized by topical painting of 4% KP and subsequent irradiation with 20 J/cm^2 UVA, or by KP alone. They were challenged on the earlobes with 2% KP and/or 20 J/cm^2 UVA. A significant ear swelling response was observed in mice challenged with both KP and UVA, whereas elicitation with KP or UVA alone did not induce the response. In mice sensitized with 4% KP alone, KP plus UVA evoked a detectable swelling response. Since elicitation with KP alone did not yield any response, this was considered to be a phototoxic response, and was significantly lower than the photoallergic response to KP. Thus, treatment with KP plus UVA was capable of inducing the allergic type of photocontact dermatitis in mice.

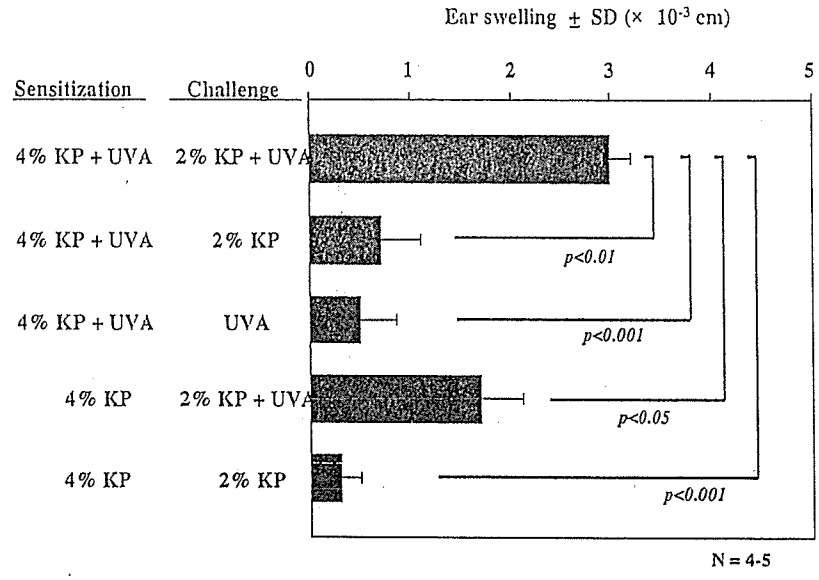

Fig. 1 Requirement of both KP and UVA for induction and elicitation of allergic photocontact dermatitis. AKR/N mice were sensitized with KP (4%) plus UVA (20 J/cm^2) or KP alone on days 0 and 1. On day 5, they were challenged on both sides of each earlobe with KP (2%) and/or subsequent UVA (20 J/cm^2). Ear swelling was measured 24 h after irradiation. Each column represents the mean ± S.D.

3.2. KP concentration and UVA dose effective for induction and elicitation of photocontact dermatitis

AKR/N and C3H/He mice were sensitized with 1, 2, or 4% KP in combination with 20 J/cm^2 UVA, and challenged with 2% KP plus 20 J/cm^2 UVA (Fig. 2A). KP at both concentrations of 2 and 4% produced significant ear swelling responses, with the latter being slightly more effective than the former. When 4% KP-photosensitized mice were challenged with 1, 2, or 4% KP in combination with 20 J/cm^2 UVA, 2 and 4% KP induced comparable responses in AKR/N mice, while all three concentrations of KP produced significant responses in C3H/He (Fig. 2B). When AKR/N mice were sensitized with 4% KP alone and challenged with 2% or 4% KP plus UVA, photochallenge with 4% KP produced two-fold higher swelling than 2% KP (data not shown), indicating that the phototoxic response of 2% KP was low.

AKR/N mice were sensitized with 4% KP and UVA at 10, 20, 30 or 40 mJ/cm^2, and challenged with 2% KP plus 20 mJ/cm^2 UVA (Fig. 2C). UVA at 20, 30, and 40 mJ/cm^2 yielded significant and comparable responses. Therefore, we used 4% KP for photosensitization and 2% KP for photochallenge in combination with 20 mJ/cm^2 UVA in the following experiments.

3.3. Different reactivity in photocontact dermatitis among various mouse strains

Eight strains of mice were sensitized and challenged with KP plus UVA. AKR/N, CBA/J, C3H/He, BALB.K/Ola, and A/J exhibited higher responses than did BALB/c, DBA/2 and B6 mice (Fig. 3). Considering that BALB/c and BALB.K/Ola mice are H-2-congenic strains and thus differ only at the H-2 complex, it seems that H-2^k mice are high responders in this sensitivity.

3.4. Adoptive transfer of photocontact dermatitis

Immune LNC were taken from AKR/N mice photosensitized with KP 5 days before and injected i.v. into naïve recipients, which were challenged with KP plus UVA. As positive control, a group of mice were epicutaneously sensitized and challenged in parallel. Fig. 4A shows that mice receiving 2 × 10^7 LNC exhibited a significant degree of photocontact dermatitis but to a lesser degree than the epicutaneously sensitized mice. Along with this study, immune LNC from BALB/c mice photosensitized with TCSA were transferred to naïve syngeneic recipients. They had a stronger but similarly reduced level of response as compared to the epicutaneously sensitized mice. When donor mice were treated with UVA alone, transfer of their LNC did not induce the sensitivity in recipients (Fig. 4B).

3.5. Essential and augmentative roles of CD4$^+$ and CD8$^+$ cells, respectively, in photocontact dermatitis

CD4$^+$ or CD8$^+$ T cells (5 × 10^6 cells/mouse) purified from KP-immune LNC of AKR/N mice were trans-

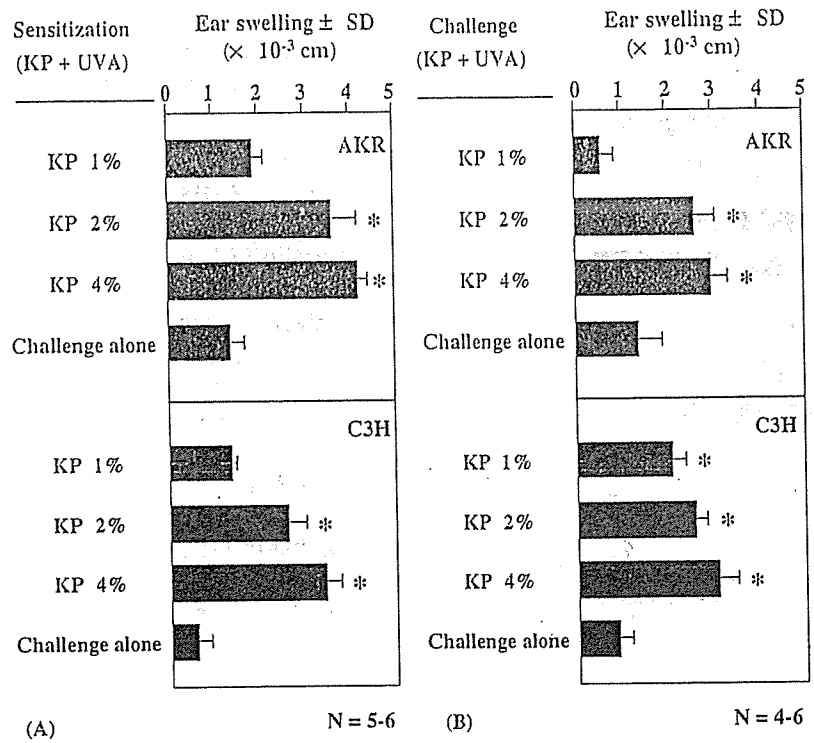

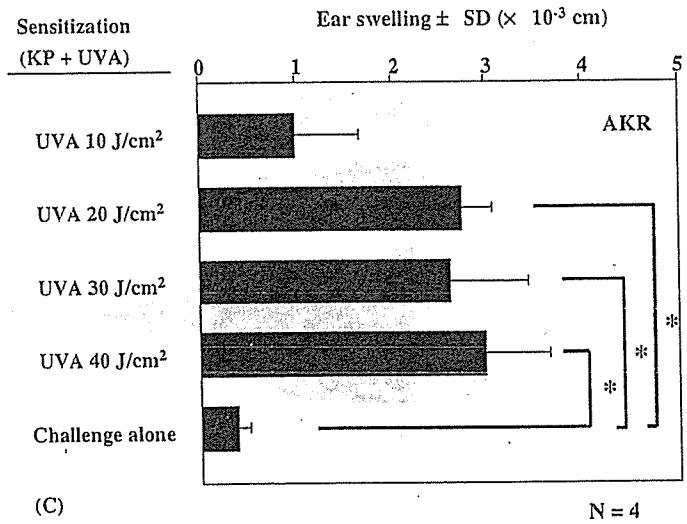

Fig. 2 Effects of KP concentration and UVA dose on sensitization and challenge of photocontact dermatitis. AKR/N and C3H/He mice were sensitized with varying doses of KP (1–4%) (A) or 4% KP (B) plus UVA (20 J/cm^2) on days 0 and 1. On day 5, they were challenged on both sides of each earlobe with 2% KP (A) or varying doses of KP (1–4%) (B) plus UVA (20 J/cm^2). In (C), AKR/N mice were sensitized with 4% KP plus varying doses (10–40 J/cm^2) of UVA and challenged with 2% KP plus 20 J/cm^2 UVA. Ear swelling was measured 24 h after irradiation. Each column represents the mean ± S.D. *$p < 0.05$.

ferred to naïve syngeneic recipients. Upon challenge with KP plus UVA, mice injected with CD4$^+$ cells, but not CD8$^+$ or CD4$^-$CD8$^-$ cells, exhibited a significant swelling response compared to the non-injected control mice (Fig. 5). When mice were injected with increasing numbers of CD8$^+$ cells additionally with CD4$^+$ cells, 5×10^6 cells, but not 1 or 2.5×10^6 cells, enhanced the CD4$^+$ cell-induced response. This combination of CD4$^+$ and CD8$^+$ cells produced a comparable response to the epicutaneously sensitized mice. The results suggested that CD4$^+$ T cells mediate the sensitivity and CD8$^+$ T cells participate in the full responses.

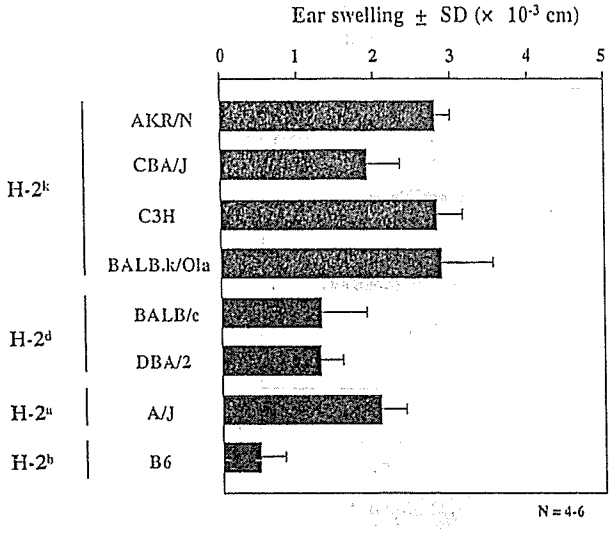

Fig. 3 Photocontact dermatitis to KP in various mouse strains with different H-2 haplotypes. Mice were sensitized with 4% KP plus 20 J/cm^2 UVA on days 0 and 1. On day 5, they were challenged with 2% KP and 20 J/cm^2 UVA. Data are expressed as: Δear swelling, representing (sensitization and challenge) − (challenge alone). Each column represents the mean ± S.D.

3.6. Elevated mRNA expression of cytokines and chemokine receptors of both Th1 and Th2 cells in immune LNC

AKR/N mice were sensitized with KP plus UVA on days 0 and 1, and single cell suspensions of immune LNC were prepared on day 1 (immediately after sensitization), 3 and 5. The expression of Th1 and Th2 cytokines, as represented by IFN-γ and IL-4, respectively, was examined by RT-PCR. As shown in Fig. 6A, KP photosensitization increased the expression of both cytokines compared to vehicle alone. Notably, IL-4 was markedly augmented by KP plus UVA on day 5.

Th1 and Th2 cells express chemokine receptor CXC chemokine receptor 3 (CXCR3) and CC chemokine receptor 4 (CCR4), respectively. The expression of these chemokine receptors was also tested in immune LNC. As most discernibly seen in day 5 LNC, CCR4 expression was remarkably enhanced by sensitization with KP plus UVA, while CXCR3 was increased to a lesser degree (Fig. 6B).

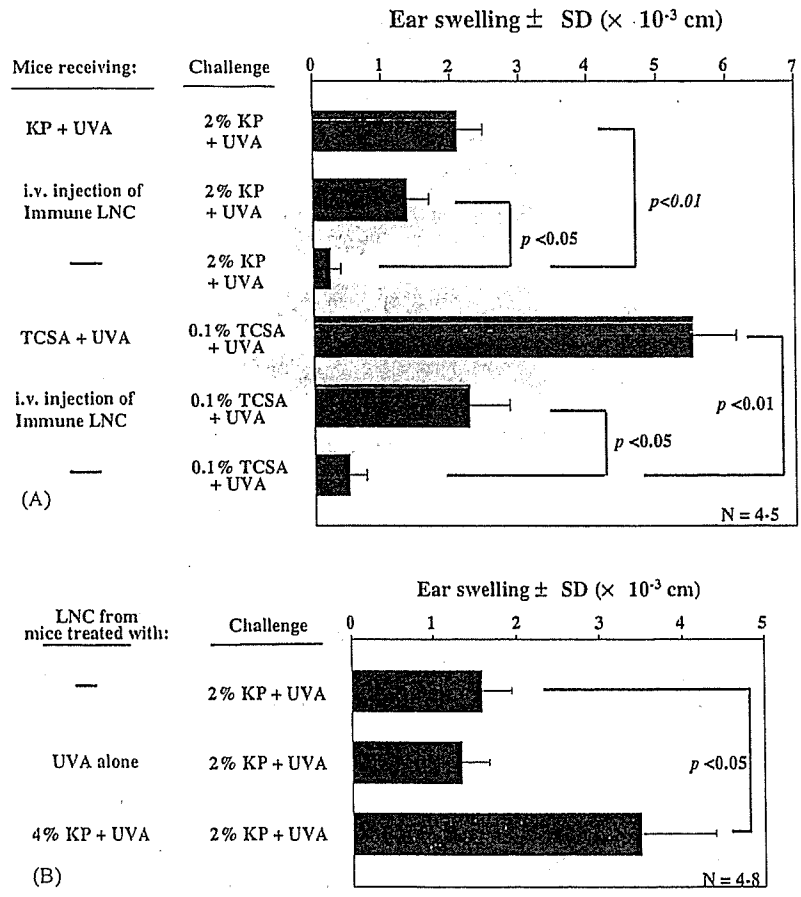

Fig. 4 (A) and (B) Transfer of LNC from KP- or TCSA-photosensitized mice. AKR/N (for KP) and BALB/c (for TCSA) mice were injected i.v. with immune LNC (2 × 10^7 cells/mouse) from KP- or TCSA-photosensitized mice. The control mice were not injected. Within 1 h after cell transfer, the recipient and control mice were challenged with 2% KP plus 20 J/cm^2 UVA or 0.1% TCSA plus 20 J/cm^2 UVA, and ear swelling response was measured after 24 h. Each column represents the mean ± S.D.

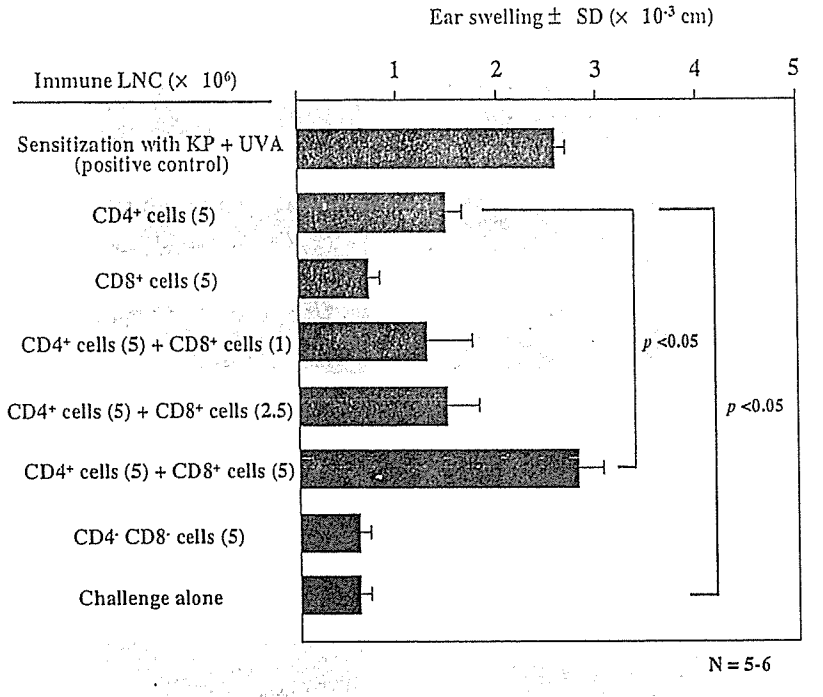

Fig. 5 Transfer of $CD4^+$ and/or $CD8^+$ cells from KP-photosensitized mice. Mice were injected with intravenous injection of purified $CD4^+$ and/or $CD8^+$ T cells from KP-photosensitized AKR/N mice. The control mice were not injected. Within 1 h after cell transfer, the recipient and control mice were challenged with 2% KP plus UVA irradiation. Each column represents the mean ± S.D.

These results suggested that Th2 cells as well as Th1 cells are stimulated in photocontact dermatitis to KP, with the former being more enhanced by this phototreatment.

3.7. Elevated mRNA expression of chemokines of both Th1 and Th2 cells in challenged epidermis

Murine epidermal keratinocytes produce Th1 chemokines, interferon-inducible protein-10 (IP-10/CXCL10) and monokine induced by interferon-γ (MIΓ/CXCL9), and Th2 chemokines, thymus and activation-regulated chemokine (TARC/CCL17) and macrophage derived chemokine (MDC/CCL22). These Th2 chemokines bind to CCR4 on Th2 cells, while the Th1 chemokines have affinity to CXCR3 on Th1 cells [15]. To address the role of these chemokines in infiltration of Th1 and Th2 cells at the challenged site, AKR/N mice were sensitized with KP and UVA, and 5 days later, challenged on the earlobes with KP or vehicle in combination with UVA. Epidermal cell suspensions were prepared from the ears 24 and 48 h after challenge and subjected to RT-PCR. At 24 h after challenge, the expression of Mig and TARC was increased by treatment with KP plus UVA, as compared to no treatment or vehicle alone (Fig. 7). The expression at 48 h was virtually the same as that at 24 h, but less discernible. IP-10 and MDC were not substantially changed. Thus, both certain Th1 and Th2 chemokines, but not all, were expressed increasingly in the challenged epidermis.

4. Discussion

The present study was aimed to establish a murine model of photocontact dermatitis to KP. The photosensitivity was successfully induced and elicited by skin application of KP and subsequent irradiation with UVA. The optimal concentration of KP was 4% for sensitization and 2% for elicitation, and the dose of UVA was 20 J/cm^2. In a comparison with a representative allergic photocontactant TCSA [3,4], these concentration and dose are high, and the degree of ear swelling response is low. Patients with photocontact dermatitis to KP exhibit a strong erythematous reaction, and even bulla formation occurs in some patients [8–11,16]. Our present system, therefore, is not a complete mimicry to the clinical photosensitivity. Nevertheless, the photoallergic potential of KP can be evaluated by this murine model.

The magnitude of response depended on the strain of mice, and at least the major histocompatibility complex (MHC) seems to influence the response. $H\text{-}2^k$ mice are high responders compared to $H\text{-}2^{d,b}$ mice. This is strikingly in contrast to photocontact dermatitis to TCSA, in which $H\text{-}2^{d,b}$ mice are high responders, while $H\text{-}2^k$ is the low

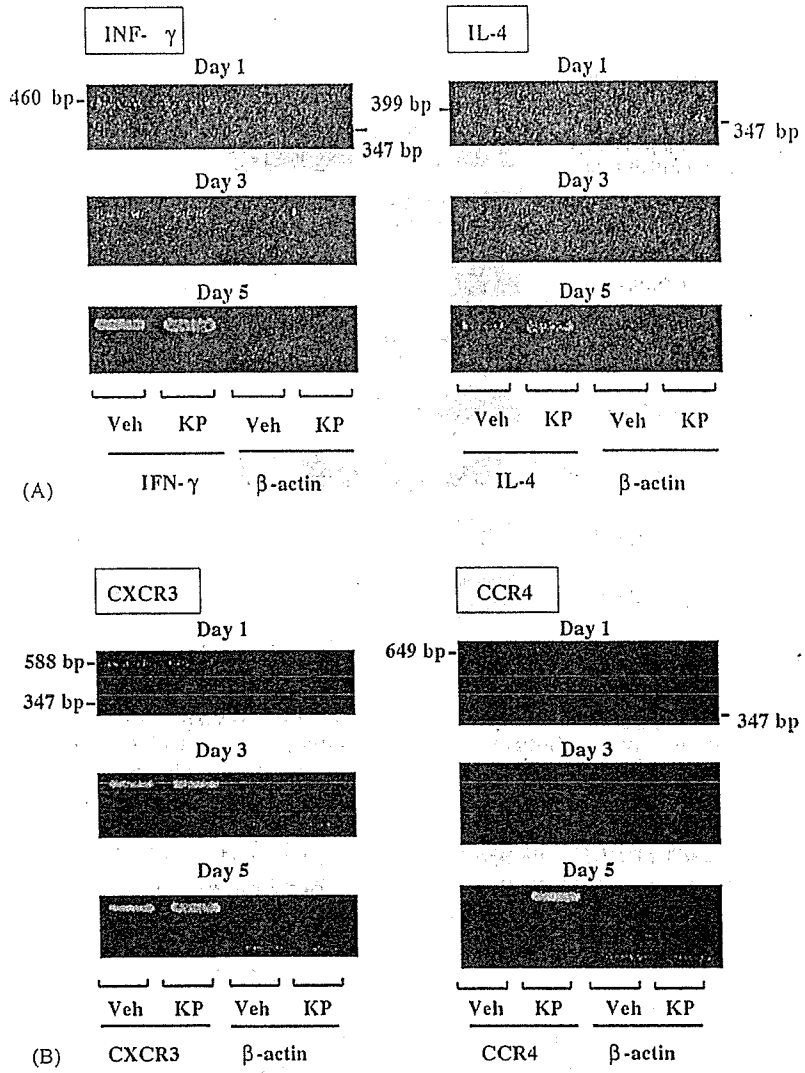

Fig. 6 RT-PCR analysis of mRNA expression of cytokines and chemokine receptors in immune LNC. LNC were taken from mice 1 h (day 1), 48 h (day 3) and 96 h (day 5) after sensitization with KP plus UVA. Each assay was performed four times using two independent samples. Representative data were shown. Veh: vehicle alone.

responder haplotype [4]. Thus, the susceptibility to photocontact dermatitis in individuals appears to be different depending on each photocontactant. The majority of exogenous photoallergic substances have a photohaptenic property [2,17]. Photohaptens are capable of binding to MHC class II molecules/self peptides on LC upon exposure to UVA [18]. In this context, the T cell response is likely controlled by MHC molecules.

In the adoptive transfer study, injection of $CD4^+$ T cells was crucial to evoke the sensitivity, but transfer of both $CD4^+$ and $CD8^+$ cells resulted in a higher response. In accordance with the present study, cutaneous photoallergy to exogenous agents is mediated by $CD4^+$ T cells [4,17,18]. The roles of $CD4^+$ and $CD8^+$ T cells in ordinary contact hypersensitivity remains disputed. Several independent studies have shown mediation of the sensitivity by $CD8^+$ T cells [19–21]. On the other hand, the contribution of $CD4^+$ cells has been variously reported, as $CD4^+$ cells are unnecessary [21], helpful [22,23], or suppressive [24,25]. Circumstantial evidence may indicate that $CD4^+$ cells participate more profoundly in photocontact hypersensitivity than ordinary contact hypersensitivity. For example, in vitro stimulation of immune LNC with photohapten results in the preferential propagation of $CD4^+$ cells, and the sensitivity can be transferred to naïve mice with $CD4^+$ T cell line [17]. In such a case, $CD8^+$ T cells may be required for the full development of the sensitivity.

In the draining LNC, mRNAs for not only IFN-γ and CXCR3 but also IL-4 and CCR4 were increasingly expressed. Rather, the expression levels of these Th2-relevant molecules were higher than those of Th1. Such a Th2 dominant state was also found in photosensitivity to TCSA [26]. In the skin, keratinocyte-derived chemokines initiate migration of T cells. mRNAs for TARC (a ligand for CCR4) and Mig

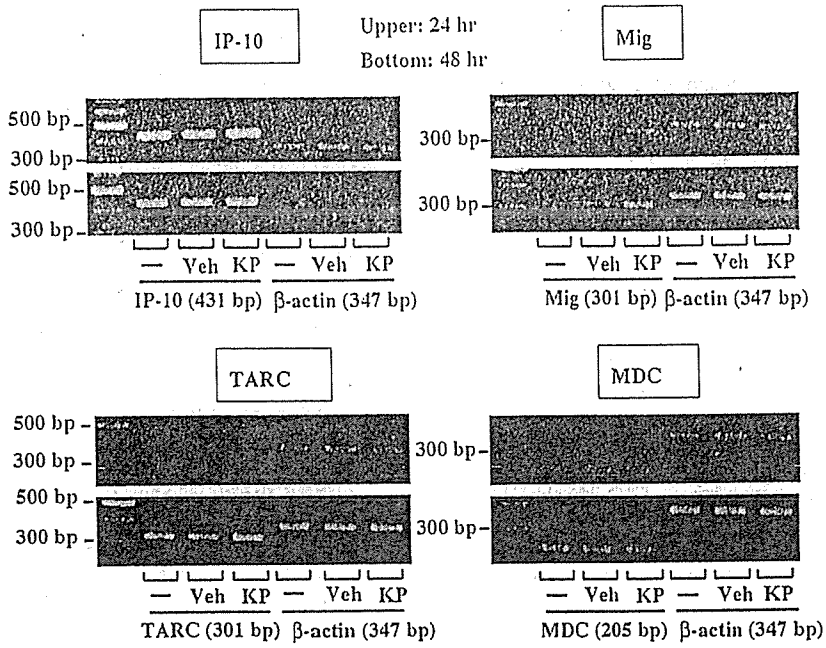

Fig. 7 RT-PCR analysis of chemokine mRNA expression in epidermal cells. Epidermal cell suspensions were prepared from earlobes of KP/UVA-sensitized mice 24 or 48 h after challenge with KP plus UVA. Each assay was performed four times using two independent samples. Veh: vehicle alone.

(a ligand for CXCR3) were also enhanced in the epidermal cells from earlobes of mice sensitized and challenged with KP plus UVA. This chemokine expression is different from that of ordinary contact sensitivity to picryl chloride, which shows apparent Th1 chemokine mRNA expression but no TARC expression in the challenged ears [27]. Of particular importance is whether these Th2 cells serve as effectors or suppressors in the sensitivity. We measured the percentage of $CD4^+CD25^+$ cells, indicative of regulatory T cells [24,25], in immune LNC from KP- or TCSA-photosensitized AKR/N or BALB/c mice, and found no increment of cells bearing this phenotype (data not shown). Together with the ability of $CD4^+$ T cells to transfer the sensitivity, these findings implies that $CD4^+$ cells play a helper or effector role in photocontact dermatitis to KP.

Photocontact dermatitis to KP is known to prolong at the applied skin site even several months after cessation of application [9–11]. This enigmatic phenomenon cannot be clarified from the present study. In addition to its photohaptenic moiety, KP might exert its pharmacological effect on LC [28], possibly leading to the prolongation. Elucidation of this phenomenon may characterize this photosensitivity more specifically.

References

[1] Tokura Y. Immunological and molecular mechanism of photoallergic contact dermatitis. J UOEH 2003;25:387–95.

[2] Tokura Y. Immune responses to photohaptens: implications for the mechanism of photosensitivity to exogenous agents. J Dermatol Sci 2000;23(Suppl):6–9.

[3] Takigawa M, Miyachi Y. Mechanisms of contact photosensitivity in mice. I. T cell regulation of contact photosensitivity to tetracholorosalicylanilide under the genetic restrictions of the major histocompatibility complex. J Invest Dermatol 1982;78:108–15.

[4] Tokura Y, Satoh T, Takigawa M, Yamada M. Genetic control of contact photosensitivity to tetrachlorosalicylanilide. I. Preferentinal activation of suppressor T cells in low responder $H\text{-}2^k$ mice. J Invest Derrmatol 1990;94:471–6.

[5] Gerberick GF, Ryan CA, Fletcher ER, Hoeard AD, Robinson MK. Increased number of dendritic cells in draining lymph nodes accompanies the generation of contact photosensitivity. J Invest Dermatol 1991;96:355–61.

[6] Yagi H, Tokura Y, Wakita H, Furukawa F, Takigawa M. TCRVβ7+ Th2 cells mediate UVB-induced suppression of murine contact photosensitivity by releasing IL-10. J Immunol 1996;156:1824–31.

[7] Bosca F, Miranda MA. Photosensitizing drugs containing the benzophenone chromophore. J Photochem Photobiol B 1998;43:1–26.

[8] Le Coz CJ, Bottlaender A, Scrivener JN, Santinelli F, Cribier BJ, Heid E, et al. Photocontact dermatitis from ketoprofen and tiaprofenic acid: cross-reactivity study in 12 consecutive patients. Contact Dermatitis 1998;38:245–52.

[9] Matsushita T, Kamide R. Five cases of photocontact dermatitis due to topical ketoprofen: photopatch testing and cross-reaction study. Photodermatol Photoimmunol Photomed 2001;17:26–31.

[10] Mozzanica N, Pigatto PD. Contact photocontact allergy to ketoprofen: clinical and experimental study. Contact Dermatitis 1990;23:336–40.

[11] Sugiura M, Hayakawa R, Xie Z, Sugiura K, Hiramoto K, Shamoto M. Experimental study on phototoxicity and the photosensitization potential of ketoprofen, suprofen, tiaprofenic acid and benzophenone and the photocross-reac-

tivity in guinea pigs. Photodermatol Photoimmunol Photomed 2002;18:82–9.
[12] Lhiaubet V, Paillous N, Chouini-Lalanne N. Comparison of DNA damage photoinduced by ketoprofen, fenofibric acid and benzophenone via electron and energy transfer. Photochem Photobiol 2001;74:670–8.
[13] Ljunggren B. Propionic acid-derived non-steroidal antiinflammatory drugs are phototoxic in vitro. Photodermatology 1985;2:3–9.
[14] Tokura Y, Yagi J, O'Malley M, Lewis JM, Takigawa M, Edelson RL, et al. Superantigenic staphylococcal exotoxins induce T-cell proliferation in the presence of Langerhans cells or class II-bearing keratinocytes and stimulate keratinocytes to produce T-cell-activating cytokines. J Invest Dermatol 1994;102:31–8.
[15] Sallusto F, Lenig D, Mackay CR, Lanzavecchia A. Flexible programs of chemokine receptor expression on human polarized T helper 1 and 2 lymphocytes. J Exp Med 1998;187:875–83.
[16] Sugiura M, Hayakawa R, Kato Y, Sugiura K, Ueda H. Four cases of photocontact dermatitis due to ketoprofen. Contact Dermatitis 2000;43:16–9.
[17] Tokura Y, Seo N, Yagi H, Furukawa F, Takigawa M. Cross-reactivity in murine fluoroquinolone photoallergy: exclusive usage of TCR Vβ13 by immune T cells that recognize fluoroquinolone-photomodified cells. J Immunol 1998;160:3719–28.
[18] Tokura Y, Seo N, Fujie M, Takigawa M. Quinolone-photoconjugated MHC class II-bearing peptides with lysine are antigenic for T cells mediating murine quinolone photoallergy. J Invest Dermatol 2001;117:1206–11.
[19] Gocinski BL, Tigelaar RE. Roles of CD4+ and CD8+ T cells in murine contact sensitivity revealed by in vivo monoclonal antibody depletion. J Immunol 1990;144:4121–8.
[20] Xu H, Banerjee A, Dilulio NA, Fairchild RL. Development of effector CD8+ T cells in contact hypersensitivity occurs independently of CD4+ T cells. J Immunol 1997;158:4721–8.
[21] Akiba H, Kehren J, Ducluzeau MT, Krasteva M, Horand F, Kaiserlian D, et al. Skin inflammation during contact hypersensitivity is mediated by early recruitment of CD8+ T cytotoxic 1 cells inducing keratinocyte apoptosis. J Immunol 2002;168:3079–87.
[22] Kondo S, Beissert S, Wang B, Fujisawa H, Kooshesh F, Stratigos A, et al. Hyporesponsiveness in contact hypersensitivity and irritant contact dermatitis in CD4 gene targeted mouse. J Invest Dermatol 1996;106:993–1000.
[23] Wang B, Fujisawa H, Zhuang L, Freed I, Howell BG, Shahid S, et al. CD4+ Th1 and CD8+ type 1 cytotoxic T cells both play a crucial role in the full development of contact hypersensitivity. J Immunol 2000;165:6783–90.
[24] Xu H, Dilulio A, Fairchild RL. T cell populations primed by hapten sensitization in contact sensitivity are distinguished by polarized patterns of cytokine production: Interferon gamma-producing (Tc1) effector CD8+ T cells and interleukin (Il) 4/Il-10-producing (Th2) negative regulatory CD4+ T cells. J Exp Med 1996;183:1001–12.
[25] Dubois B, Chapat L, Goubier A, Papiernik M, Nicolas JF, Kaiserlian D. Innate CD4+ CD25+ regulatory T cells are required for oral tolerance and control CD8+ T cells mediating skin inflammation. Blood 2003;102:3295–32301.
[26] Suzuki K, Yamazaki S, Tokura Y. Expression of T-cell cytkines in challenged skin of murine allergic contact photosensitivity: low responsiveness in associated with induction of Th2 cytokines. J Dermatol Sci 2000;23:138–44.
[27] Tokuriki A, Seo N, Ito T, Kumakiri M, Takigawa M, Tokura Y. Dominant expression of CXCR3 is associated with induced expression of IP-10 at hapten-challenged sites of murine contact hypersensitivity: a possible role for interferon-gamma-producing CD8(+) T cells in IP-10 expression. J Dermatol Sci 2002;28:234–41.
[28] Kabashima K, Sakata D, Nagamachi M, Miyachi Y, Inaba K, Narumiya S. Prostaglandin E2-EP4 signaling initiates skin immune responses by promoting migration and maturation of Langerhans cells. Nat Med 2003;9:744–9.